# Microglia Induce Motor Neuron Death via the Classical NF-κB Pathway in Amyotrophic Lateral Sclerosis

Ashley E. Frakes,[1,2] Laura Ferraiuolo,[1] Amanda M. Haidet-Phillips,[1,5] Leah Schmelzer,[1] Lyndsey Braun,[1] Carlos J. Miranda,[1] Katherine J. Ladner,[3] Adam K. Bevan,[1,2] Kevin D. Foust,[4] Jonathan P. Godbout,[4] Phillip G. Popovich,[4] Denis C. Guttridge,[3] and Brian K. Kaspar[1,2,4,*]

[1]Center for Gene Therapy, The Research Institute at Nationwide Children's Hospital, Columbus, OH 43205, USA
[2]Biomedical Sciences Graduate Program, College of Medicine
[3]Department of Molecular Virology, Immunology and Medical Genetics
[4]Department of Neuroscience
The Ohio State University, Columbus, OH 43210, USA
[5]Present address: Department of Neurology, Johns Hopkins University School of Medicine, Baltimore, MD 21205, USA
*Correspondence: Brian.Kaspar@NationwideChildrens.org
http://dx.doi.org/10.1016/j.neuron.2014.01.013

## SUMMARY

Neuroinflammation is one of the most striking hallmarks of amyotrophic lateral sclerosis (ALS). Nuclear factor-kappa B (NF-κB), a master regulator of inflammation, is upregulated in spinal cords of ALS patients and SOD1-G93A mice. In this study, we show that selective NF-κB inhibition in ALS astrocytes is not sufficient to rescue motor neuron (MN) death. However, the localization of NF-κB activity and subsequent deletion of NF-κB signaling in microglia rescued MNs from microglial-mediated death in vitro and extended survival in ALS mice by impairing proinflammatory microglial activation. Conversely, constitutive activation of NF-κB selectively in wild-type microglia induced gliosis and MN death in vitro and in vivo. Taken together, these data provide a mechanism by which microglia induce MN death in ALS and suggest a novel therapeutic target that can be modulated to slow the progression of ALS and possibly other neurodegenerative diseases by which microglial activation plays a role.

## INTRODUCTION

Amyotrophic lateral sclerosis (ALS) is a devastating, fast-progressing neurodegenerative disease characterized by motor neuron (MN) death in the brainstem, spinal cord, and motor cortex. Typically within 2–5 years of clinical onset, patients succumb to the disease due to severe muscle atrophy, paralysis, and ultimately denervation of respiratory muscles. Most ALS cases are classified as sporadic, defined as having no family history of the disease. The remaining 5%–10% of cases are classified as familial and are typically inherited in an autosomal dominant fashion. Despite genetic differences, these two forms of ALS are clinically indistinguishable. Approximately 20% of familial

cases are associated with mutations in the gene superoxide dismutase 1 (SOD1) (Rosen et al., 1993). Transgenic rodents carrying mutant forms of SOD1 develop a similar, progressive MN disease akin to patients and are used as the gold standard in ALS research. Elegant studies using these animals have shown that nonneuronal cells play a crucial role in ALS, contributing to MN death via non-cell-autonomous mechanisms (Clement et al., 2003). Similarly, in vitro studies have shown that murine astrocytes and microglia expressing mutant SOD1 and human astrocytes from sporadic and familial ALS patients can induce MN death (Di Giorgio et al., 2007, 2008; Haidet-Phillips et al., 2011; Marchetto et al., 2008; Nagai et al., 2007; Xiao et al., 2007). Evidence that individual cell types mediate different aspects of disease emerged from the generation of mice expressing a conditional deletion of the mutant SOD1 gene. Removal of mutant SOD1 specifically in MNs extended survival by delaying disease onset and early disease progression, while excising floxed mutant SOD1 in either microglia/macrophages or astrocytes extended survival by slowing disease progression, but not onset (Boillée et al., 2006; Yamanaka et al., 2008). Similarly, replacing the myeloid lineage of mutant SOD1 mice with wild-type (WT) microglia/macrophages slowed disease progression (Beers et al., 2006). This suggests ALS is a deadly convergence of damage developed in multiple cellular compartments that ultimately leads to neuromuscular failure. However, the precise mechanisms by which individual cell types such as astrocytes and microglia contribute to the disease remain unknown.

One of the most striking hallmarks of ALS shared by familial and sporadic patients, as well as by rodent models, is neuroinflammation, characterized by extensive astrogliosis, microglial activation, and infiltration of peripheral immune cells at sites of neurodegeneration (Alexianu et al., 2001; Hall et al., 1998; Kawamata et al., 1992; Mantovani et al., 2009; Turner et al., 2004). Mutant SOD1 astrocytes and microglia exhibit increased expression of many proinflammatory genes (Philips and Robberecht, 2011). However, genetic approaches to globally eliminate single inflammatory genes in ALS mouse models have largely failed to extend survival (Almer et al., 2006; Gowing et al., 2006; Nguyen

et al., 2001; Son et al., 2001) and in some cases have even hastened disease progression (Lerman et al., 2012), highlighting the complexity of neuroinflammation in ALS. For these reasons, a successful therapeutic approach is likely to derive from a better understanding of the intricate molecular mechanisms driving the inflammatory response and the identification of upstream transcription factors that are dysregulated in each cellular compartment throughout the course of disease.

Classical NF-κB signaling involving the p65/p50 heterodimer is a major regulator of inflammation, driving gene expression of proinflammatory cytokines, chemokines, enzymes, and adhesion molecules, many of which are upregulated in ALS. When inflammatory mediators bind their respective receptors, a signaling cascade is initiated that leads to phosphorylation and activation of IKKβ (a subunit of the inhibitor of *IκB kinase* [IKK] complex). Activated IKKβ phosphorylates the IκB inhibitory protein IκBα, targeting it for ubiquitination and proteasomal degradation and subsequent release of NF-κB (p65/p50) to the nucleus where it binds to its cognate DNA sequences to induce gene expression (Ghosh and Karin, 2002). Additionally, phosphorylation by IKKβ at specific serine residues is required for transactivation function of the p65 subunit of NF-κB (Hayden and Ghosh, 2008). We previously reported NF-κB as the highest-ranked regulator of inflammation by Ingenuity Pathway Analysis of inflammatory gene array data from astrocytes derived from human postmortem ALS patients (Haidet-Phillips et al., 2011). Other laboratories have confirmed by immunohistochemistry that NF-κB is activated in glia in familial and sporadic ALS patients (Swarup et al., 2011). Interestingly, loss-of-function mutations in the gene optineurin, which is known to negatively regulate TNF-α-induced NF-κB activation, have been found in ALS patients (Maruyama et al., 2010). However, it remains unknown whether NF-κB activation in ALS glia is involved in MN death.

Since the role of glial-derived inflammation in ALS remains ambiguous, we sought to determine whether inflammatory signaling regulated by NF-κB in astrocytes and microglia mediates MN death in ALS. In the current study, we demonstrate that NF-κB is activated with disease progression in the SOD1-G93A mouse model, specifically in glia. In agreement with recent publications, inhibition of NF-κB in astrocytes, using both transgenic and viral-mediated gene delivery approaches, did not increase motor function or survival in our SOD1-G93A mice (Crosio et al., 2011). However, inhibition of NF-κB selectively in microglia rescues MN survival in vitro, and, in vivo, extends survival in the ALS mice by delaying disease progression by 47%, one of the longest extensions reported in this severe model. NF-κB inhibition in microglia leads to marked reduction in prototypic inflammatory markers, suggesting that NF-κB regulates microglial conversion to a proinflammatory, neurotoxic state in ALS. Conversely, we show that constitutive activation of NF-κB selectively in myeloid cells in WT mice creates the pathological features of ALS in the spinal cord (i.e., gliosis and MN death). Together, these data indicate that NF-κB activation in microglia is a novel molecular mechanism underlying MN death in ALS. Moreover, the data identify a new therapeutic target to modulate microglial activation and slow the progression of ALS and possibly other neurodegenerative diseases in which microglial activation plays a role.

## RESULTS

### NF-κB Is Activated with Disease Progression in the SOD1-G93A Mouse Model of ALS

In order to gain insight into NF-κB regulation in ALS, we performed electrophoretic mobility shift assay (EMSA) analysis on whole-spinal-cord nuclear lysates from the SOD1-G93A mouse model. NF-κB DNA binding activity was increased in end-stage ALS mice compared to WT littermates (Figure S1A available online). Supershift EMSA analysis revealed the binding contribution of p65 (Figure S1B). Interestingly, we were unable to show a supershift using antisera against p50, c-Rel, and RelB subunits, which may be more of a limitation of the antibody than the lack of presence of these NF-κB subunits in spinal cords of SOD1-G93A mice. To investigate the extent of p65-mediated classical NF-κB activation in the SOD1-G93A mouse model at different stages of disease, whole-lumbar spinal cord protein was analyzed for the transcriptionally active, phosphorylated form of p65 from three SOD1-G93A female mice at the presymptomatic stage (pre-sym), disease onset, symptomatic (sym), late-symptomatic (late-sym), and end-stage (ES). We found that as diseased progressed in ALS animals, phospho-p65 levels increased modestly from pre-sym to sym, although fold changes were not statistically significant. However, at late-sym, phospho-p65 levels were 13.7-fold greater in SOD1-G93A mice compared to WT and 8.7-fold greater than WT at ES (Figures 1A and 1B). In order to determine whether the increase in phospho-p65 levels observed at late-sym stages is statistically different compared to the levels at ES, we analyzed lumbar spinal cord lysates from additional late-sym (n=6) and ES SOD1-G93A mice (n=6), revealing no statistical difference in NF-κB activation between late-sym and ES (Figures S1C and S1D). To determine the contribution of astrocytes to this increase, we isolated primary astrocytes from the spinal cords of WT and SOD1-G93A mice at the late-sym stage. Western blot analysis showed a 4.4-fold increase in phospho-p65 in ALS astrocytes compared to WT (Figure 1C).

### NF-κB Inhibition in Astrocytes Does Not Confer Neuroprotection In Vitro or In Vivo in the SOD1-G93A Mice

To determine the relevance of NF-κB activation to astrocyte-mediated MN death in ALS, we tested NF-κB inhibition in an in vitro coculture model of familial ALS. We utilized an embryonic stem cell line containing an Hb9-GFP reporter, which we and others have shown recapitulate aspects of MN pathology and cell death when cocultured with ALS glia (Di Giorgio et al., 2007; Haidet-Phillips et al., 2011; Nagai et al., 2007; Wichterle et al., 2002). After 5 days in coculture, the number of MNs present on SOD1-G93A astrocytes was statistically reduced by 49% compared to the MNs surviving on WT astrocytes (Figure S2A). To test the role of NF-κB in SOD1-G93A astrocytes, we utilized an adenovirus expressing the transdominant super repressor inhibitor of NF-κB (IκBα-SR). IκBα-SR is an IκBα mutant that is resistant to phosphorylation-induced degradation, thus blocking phosphorylation sites of p65 and inhibiting transcriptional function of the NF-κB complex (Wang et al., 1999). We confirmed that adenoviral vectors were capable of targeting
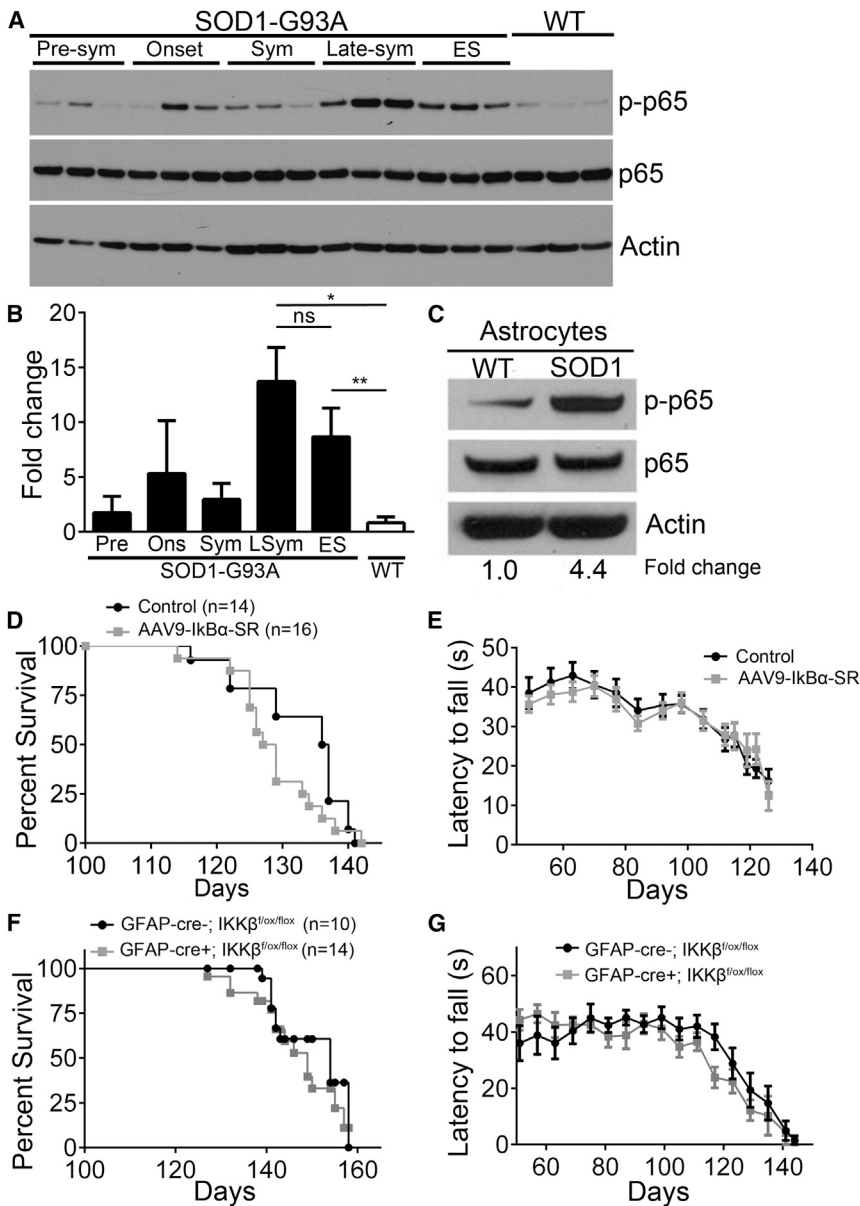
**Figure 1. The Classical NF-κB Pathway Is Activated with Disease Progression in the SOD1-G93A Mouse Model and Astroglial NF-κB Inhibition Does Not Confer Neuroprotection**

(A and B) Immunoblot (A) and fold changes (B) of lumbar spinal cord protein isolated from WT mice at 120 days and from SOD1-G93A female mice at presymptomatic (Pre-sym), onset (Onset), symptomatic (Sym), late-symptomatic (Late-sym), and end-stage (ES). Phospho-p65 (top) total p65 (middle) and Actin (bottom). n=3. Additional data shown in Figure S1.

(C) Immunoblot of protein isolated from astrocytes obtained from late-sym SOD1-G93A and WT littermates.

(D and E) Kaplan-Meier survival curve (D) of SOD1-G93A mice injected with AAV9-IκBα-SR (median survival=128; n=16) and noninjected controls (median survival=136.5; n=14) and motor performance on accelerating rotarod test (E).

(F and G) Kaplan-Meier survival curve (F) of SOD1-G93A; IKKβ[f/f]; GFAP-cre− (median survival=154; n=10) and SOD1-G93A; IKKβ[f/f]; GFAP-cre+ mice (median survival=149; n=14) and motor performance on accelerating rotarod test (G). All band intensities were normalized to p65/Actin. Error bars represent SEM. *p<0.05; **p<0.01. See also Figures S1 and S2.

natal day 60 to preferentially target >50% astrocytes in the CNS (Foust et al., 2009, 2013). Consistent with the in vitro data above, overexpression of IκBα-SR in astrocytes utilizing AAV9 neither altered survival nor improved motor performance in the SOD1-G93A mice compared to noninjected controls (Figures 1D and 1E) or SOD1-G93A mice injected with AAV9-GFP (Foust et al., 2013).

To transgenically inhibit NF-κB in astrocytes in SOD1-G93A mice, we mated SOD1-G93A mice to mice with conditional mutants of IKKβ (IKKβ[f/f]), which have exon 3 of the *ikbkb* (IKKβ) gene flanked by loxP

nearly 100% of astrocytes in vitro (data not shown) (Miranda et al., 2012). However, overexpression of IκBα-SR in SOD1-G93A astrocytes did not rescue MN death in vitro, despite being functional and decreasing phospho-p65 levels (Figures S2A and S2B). In fact, there were fewer MNs surviving after 4 days in coculture with SOD1-G93A astrocytes overexpressing IκBα-SR compared to SOD1-G93A astrocytes; however, significance was lost on subsequent days (Figure S2A).

Since our in vitro model may not fully recapitulate all aspects of astrocyte-induced pathology in ALS, we simultaneously tested NF-κB inhibition in vivo using two independent, cell-type-specific approaches: viral-mediated gene delivery and transgenic cre-lox recombination. As a therapeutically relevant study, we injected SOD1-G93A mice with adeno-associated viral vector serotype 9 (AAV9) to deliver IκBα-SR. Mice were injected at post-

sites (Li et al., 2003; Park et al., 2002). We crossed these mice to a strain expressing cre recombinase under the regulation of the glial fibrillary acidic protein (GFAP) promoter, thus ablating IKKβ and downstream NF-κB activity specifically in astrocytes. We confirmed cre expression was restricted to GFAP-expressing astrocytes in the spinal cord by crossing GFAP-cre mice to a Rosa26 line that expresses tdTomato (RFP) in all cre-expressing cells (Figure S2C). We observed robust RFP expression in GFAP+ and EAAT2+ cells (Figure S2D); RFP expression was absent in Iba-1+ microglia as well as in ChAT+ neurons in the spinal cord as previously reported (Figure S2C) (Yamanaka et al., 2008; Zhuo et al., 2001). Immunoblot of lumbar spinal cord protein demonstrated a 58% reduction in phospho-p65 levels in SOD1; IKKβ[f/f]; GFAP-cre+ mice compared to SOD1 cre− mice at the symptomatic stage of disease (Figure S2E). Despite the

reduction in phospho-p65, motor impairment and survival in the GFAP-cre+ mice were not improved compared to GFAP-cre-negative controls (Figures 1F and 1G). Indeed, our findings are consistent with a recent study crossing ALS mice to a strain overexpressing IκBα-SR under the GFAP promoter (Crosio et al., 2011).

### NF-κB Activation Occurs Predominately in Microglia in the SOD1-G93A Mouse Model

To evaluate whether astrocytes are the main cells contributing to the increase in lumbar NF-κB activation, we crossed the SOD1-G93A mice to a NF-κB-GFP reporter mouse strain that expresses GFP under the control of NF-κB *cis* elements (Magness et al., 2004). Since robust NF-κB activation in SOD1-G93A was evident at late stages of disease in lumbar spinal cord protein, we analyzed lumbar spinal cord sections from late-sym SOD1; NF-κB-GFP mice for GFP expression. We observed a population of bright GFP+ cells identified as microglia by overlapping confocal Iba-1 staining (Figure 2A). We also observed a dim GFP+ population of GFAP+ astrocytes (Figure 2B). We confirmed these findings by analyzing phospho-p65 levels in protein from microglia isolated from late-sym SOD1-G93A mice. Impressively, phospho-p65 was 12.4-fold greater in SOD1-G93A microglia than WT microglia (Figure 2C). To determine the time course of NF-κB activation in microglia as disease progressed, we performed immunohistochemistry of SOD1; NF-κB-GFP lumbar spinal cord sections at pre-sym, onset, sym, late-sym, and ES. We observed that majority of bright and dim GFP+ cells colocalized with the microglial marker tomato lectin at disease onset with an increase in the number and GFP intensity as disease progressed, coinciding with microglial activation and gliosis (Figures 2D and 2E). These data reveal that microglia contribute to the robust NF-κB activation that occurs during ALS disease progression.

### Adult SOD1-G93A Microglia Are Toxic to MNs In Vitro

To study the mechanisms by which microglia mediate MN death in ALS and the contribution of NF-κB activation to this process, we sought to establish an in vitro coculture model of ALS. We found no difference in MN survival when MNs were cocultured with SOD1-G93A primary neonatal microglia compared to WT (Figure S3), suggesting these young cells were not recapitulating important aspects of the adult-onset neurodegenerative disease. Therefore, we established a coculture utilizing primary adult microglia isolated from symptomatic ALS mice. We utilized a previously described method that combines density separation and culture selection (Moussaud and Draheim, 2010). Immunocytochemical characterization of adult microglia obtained by this method showed that microglia were positive for prototypic microglial markers including Iba-1, CD11b, and F4/80 and negative for GFAP, ChAT, and NG2 (Figures 3A and 3B). Flow cytometry confirmed that this technique yields a homogenous population of microglia (Figure 3C). We observed no difference in our assays when we used spinal-cord- or brain-derived microglia; therefore, to decrease the number of animals used, we performed experiments using brain microglia.

To determine the capacity for SOD1-G93A adult microglia to induce MN death, we cocultured WT Hb9:GFP+ MNs with WT or SOD1-G93A microglia. After 72 hr, MN numbers decreased 50% when cocultured with SOD1-G93A microglia compared to WT microglia (Figures 3D and 3E). To confirm that MN death is specific to the causative SOD1 mutation, we overexpressed a shRNA targeting the human SOD1 transgene in the SOD1-G93A microglia by lentivirus, shown to reduce mutant protein by 75% (Figure 3F). When mutant SOD1 protein was reduced in SOD1-G93A microglia, MNs survival was rescued (Figures 3D and 3E).

### Adult SOD1-G93A Microglia Induce MN Death in an NF-κB-Dependent Mechanism In Vitro

To examine whether NF-κB activation in microglia is involved in MN death in vitro, we employed two independent approaches to abolish NF-κB activation in microglia. First, we overexpressed IκBα-SR via adenovirus (Ad-IκBα-SR) in SOD1-G93A and WT microglia. We also used a genetic approach by isolating microglia from SOD1-G93A; IKKβ^f/f mice and infecting the microglia in vitro with an adenovirus expressing cre recombinase (Ad-cre) to remove IKKβ^f/f in microglia postisolation. After 12 hr, we observed no difference in survival or axon length of the MNs cocultured with SOD1-G93A or WT microglia (Figure 4A). However, after 72 hr of coculture there was a 61% reduction in MN survival and marked reduction in axon length when MNs were cocultured with SOD1-G93A microglia compared to WT (Figure 4B). Live imaging of these cocultures captures the dynamic nature of microglia and rapid MN death induced by SOD1-G93A microglia (Movies S1 and S2). Initially, WT microglia phagocytosed MN debris generated from the FACS sorting and plating. WT microglia then proceeded to actively survey synapses of MNs, not disrupting intact synapses. On the contrary, SOD1-G93A microglia assaulted intact synapses, thus causing axonal damage and MN death, finishing with phagocytosis of the neuronal debris. Remarkably, NF-κB inhibition, either transgenically or by overexpression of IκBα-SR, fully rescued MN axon length and survival in vitro to WT levels (Figures 4A and 4B). Live imaging shows SOD1-G93A microglia with NF-κB inhibition preserved intact MNs similar to WT microglia (Movies S3 and S4). We evaluated the efficiency of NF-κB induction by measuring nitric oxide (NO) and TNF-α levels in the coculture medium, both of which are products of classical NF-κB activation and inflammatory microglia (Ghosh and Karin, 2002). TNF-α levels decreased by 45% and by 64% when NF-κB was inhibited in SOD1-G93A microglia using Ad-IκBα-SR and Ad-cre, respectively (Figure 4C). NO levels were reduced by 71% and by 56% in SOD1-G93A microglia using Ad-IκBα-SR and Ad-cre, respectively (Figure 4D). Corresponding with TNF-α and NO levels, phospho-p65 was reduced by 79% and 81% using Ad-IκBα-SR and Ad-cre, respectively, compared to SOD1-G93A microglia (Figure 4E). To confirm NF-κB transcriptional activity was reduced with Ad-IκBα-SR and Ad-cre, we performed an NF-κB luciferase assay. Firefly luciferase activity normalized to renilla luciferase was 6.2-fold greater in SOD1-G93A microglia compared to WT, and Ad-IκBα-SR and Ad-cre both reduced NF-κB-dependent luciferase activity in SOD1-G93A microglia to near WT levels (Figure 4F). These data suggest that SOD1-G93A microglia induce MN death in an NF-κB-dependent mechanism.
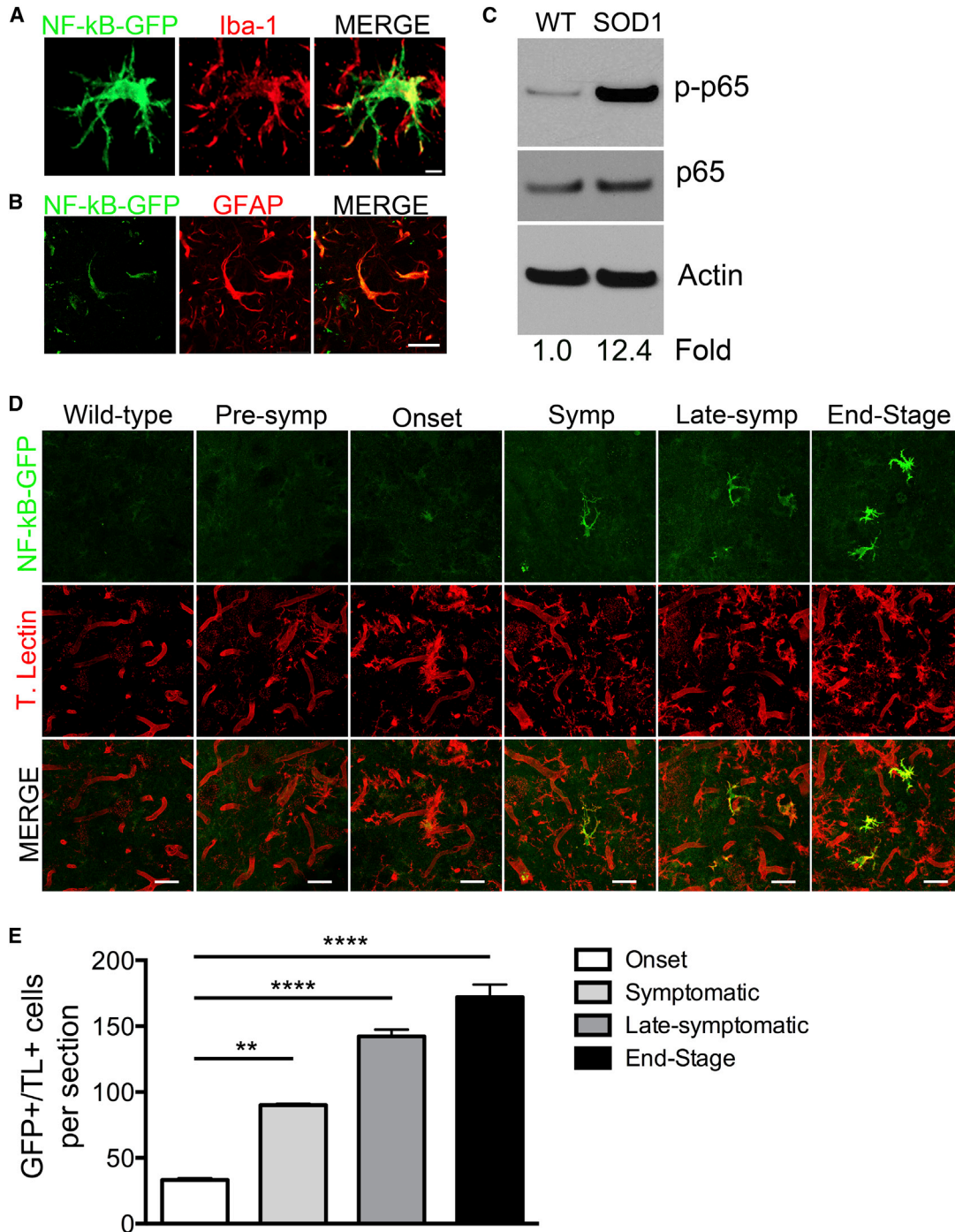
**Figure 2. NF-κB Activation Occurs Predominately in Microglia in the SOD1-G93A Mouse Model**

(A and B) Representative high-magnification images of NF-κB-GFP-positive cells (green) in the lumbar ventral horn of late-symptomatic NF-κB EGFP;SOD1-G93A mice. Most predominant GFP+ cells (A) also positive for microglial marker Iba1 (red). Other GFP+ cells positive for astrocyte maker GFAP (blue). Scale bar indicates 5 μm in (A) and 20 μm in (B).

(C) Immunoblot of protein isolated from primary microglia obtained from late-sym SOD1-G93A mice and WT littermates. Fold change determined by phospho-p65 band intensity normalized to p65/Actin.

(D) Immunohistochemistry of lumbar ventral horn of WT; NF-κB -GFP at 120 days and SOD1-G93A; NF-κB -GFP mice pre-sym, onset, sym, late-sym, and ES. NF-κB activation shown by NF-κB EGFP (green), and microglia and vasculature shown by tomato lectin (red). Scale bar indicates 50 μm.

(E) Quantification of GFP+ cells colocalizing with tomato lectin in lumbar spinal cord sections of SOD1-G93A; NF-κB -GFP mice. Error bars represent SEM. **p<0.01; ****p< 0.0001.
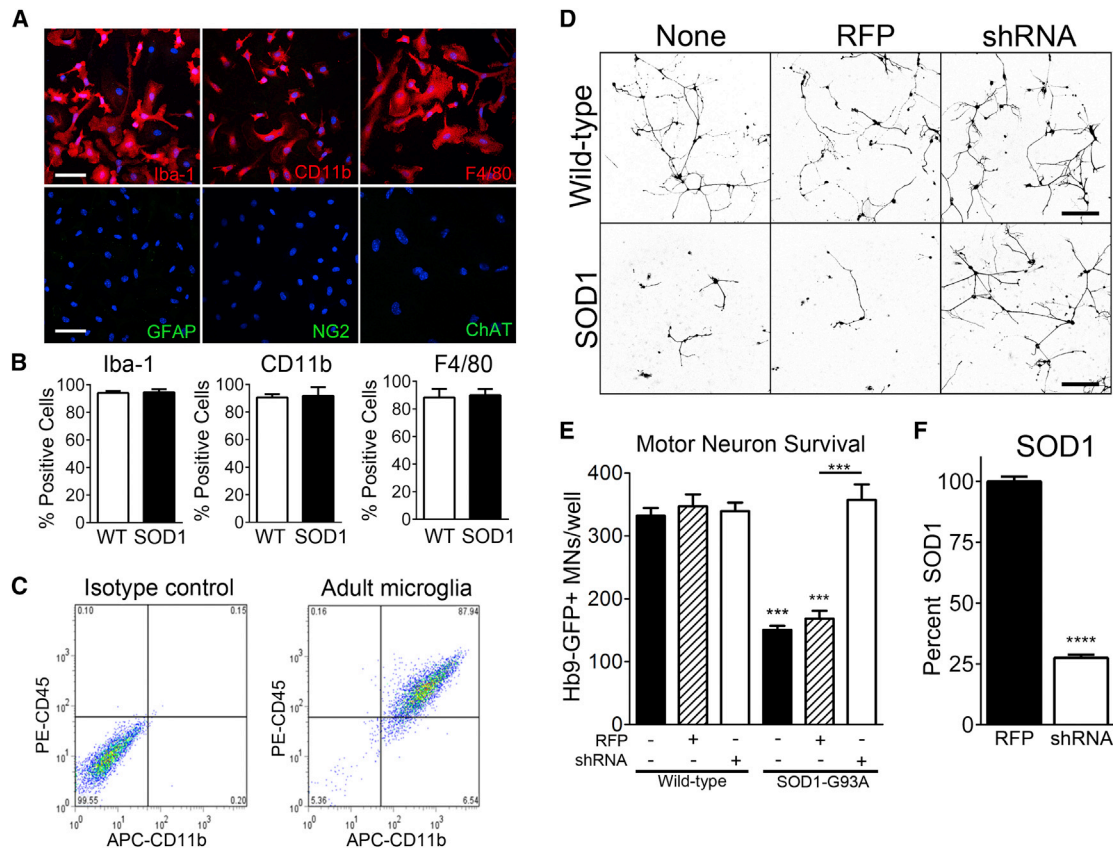
**Figure 3. Adult SOD1-G93A Microglia Are Toxic to MNs In Vitro**

(A and B) Immunocytochemistry of WT and SOD1-G93A microglia for prototypic microglial markers Iba-1, CD11b, and F4/80 and astrocytes (GFAP), oligodendrocyte precursors (NG2), and MNs (ChAT). Quantification per well (B). DAPI (blue) Scale bar indicates 20 μm.

(C) Flow cytometry of adult microglia for CD45 and CD11b.

(D and E) Representative microscopic field (D) and quantification of well (E) of surviving Hb9-GFP+ MNs after 3 days (72 hr) of coculture with either WT or SOD1-G93A microglia that were not infected (black bars) or infected with Lv-RFP (dashed bars) or Lv-shRNA-SOD1 (white bars). Scale bar indicates 200 μm.

(F) Quantification of human SOD1 protein in SOD1-G93A microglia infected with Lv-RFP and Lv-shRNA-SOD1 determined by ELISA. Error bars represent SEM. ***p< 0.001; ****p<0.0001. See also Figure S3.

## SOD1-G93A Microglia Induce MN Death in an NF-κB-Dependent Mechanism In Vivo

Since we have established that (1) NF-κB activation during the disease course in SOD1-G93A mice occurs in microglia (Figure 2) and (2) SOD1-G93A microglia kill MNs in vitro via an NF-κB-dependent mechanism (Figure 4), we tested the hypothesis that NF-κB inhibition in microglia would attenuate disease in SOD1-G93A mice. To do so, we crossed SOD1-G93A; IKKβ$^{f/f}$ mice to mice expressing cre recombinase driven by the promoter for the gene *c-fms*, which encodes *C*olony *s*timulating *f*actor *r*eceptor 1 (CSF-1R). As shown by MacGreen reporter mice that express GFP under the regulation of the *c-fms* promoter, CSF-1R is expressed throughout the mononuclear phagocyte system of the mouse, but only microglia express CSF-1R in the postnatal mouse brain (Erblich et al., 2011; Sasmono and Williams, 2012; Sasmono et al., 2003). To confirm cell-type specificity of cre expression driven by the *c-fms* (CSF-1R) promoter, we crossed CSF-1R-cre mice to the Rosa26-Td-Tomato mouse strain. We observed RFP expression only in Iba-1-positive microglia in the adult mouse spinal cord,

and RFP expression was absent in MNs and astrocytes (Figures S4A and S4B).

Mice homozygous for IKKβ (IKKβ$^{f/f}$), both SOD1 and WT, displayed serious immune dysfunction, such as enlarged spleens, eye infections, and missing or very brittle teeth, which have been previously reported in mice with myeloid cells devoid of NF-κB (Ruocco et al., 2005; Vallabhapurapu and Karin, 2009). These mice could not be maintained in the colony long enough to evaluate survival; thus, we analyzed IKKβ$^{f/wt}$ heterozygous mice. To determine the efficiency of IKKβ knockdown in these heterozygotes, immunohistochemistry was performed probing for IKKβ in lumbar spinal cord sections from SOD1-G93A; IKKβ$^{f/wt}$; CSF-1R-cre+ and cre− mice. SOD1-G93A; IKKβ$^{f/wt}$; CSF-1R-cre+ showed a decrease in IKKβ staining compared to cre negative controls (Figure S4C). To ensure knock down was specific for IKKβ, we evaluated IKKγ, the regulatory subunit of the IKK signaling complex, and observed no difference between CSF-1R-cre+ and cre− mice (Figure S4C). Remarkably, reducing IKKβ, and thus NF-κB activation, resulted in a pronounced 20 day extension in median survival in SOD1-G93A;

IKKβ[f/wt]; CSF-1R-cre+ mice compared to cre− controls (133 days in cre− and 153 days in cre+) (Figure 5A). While disease onset was not altered (102.8 ± 1.1 days in cre− and 101.1 ± 1.3 days in cre+), disease progression was significantly extended by 47% in cre+ mice compared to cre− mice (34.8 ± 1.4 days in cre− and 51.1.1 ± 1.7 days in cre+) (Figures 5B and 5C). Video of age-matched littermates show SOD1-G93A; IKKβ[f/wt]; CSF-1R-cre+ mouse able to ambulate around cage while the SOD1-G93A; IKKβ[f/wt]; CSF-1R-cre− littermate is at ES (Movie S5). To confirm the level of NF-κB inhibition that was achieved to slow disease progression by 47%, we analyzed lumbar spinal cord protein for phospho-p65 from SOD1-G93A; IKKβ[f/wt]; CSF-1R-cre+ or cre− mice at ES. Remarkably, phospho-p65 was reduced by 44% in SOD1-G93A; IKKβ[f/wt]; CSF-1R-cre+ mice compared to cre− SOD1 controls, which expressed 7.5-fold more phospho-p65 than WT controls. This is consistent with the 40% decrease in IKKβ we observed in SOD1-G93A; IKKβ[f/wt]; CSF-1R-cre+ mice compared to cre− controls (Figure 5D). Notably, NF-κB inhibition did not reduce the levels of mutant SOD1 in CSF-1R-cre+ mice compared to cre− SOD1 control mice (Figure 5D).

To determine the impact of NF-κB inhibition on astrogliosis and microgliosis, we analyzed lumbar spinal cord sections by immunohistochemistry for intensity of GFAP and Iba-1, respectively. No difference in gliosis could be detected between ES SOD1-G93A; IKKβ[f/wt]; CSF-1R-cre+ and cre− mice (data not shown). However, considering that SOD1-G93A; IKKβ[f/wt]; CSF-1R-cre+ mice endured disease for an additional 3 weeks compared to controls, it is possible that differences in gliosis achieved earlier in disease are lost at ES. Indeed, when we sacrificed the SOD1-G93A; IKKβ[f/wt]; CSF-1R-cre+ mice at the same age as the cre− littermate controls reached endpoint, we observed a significant decrease in signal intensity of GFAP by 31% and of Iba-1 by 25%, indicating astrogliosis and microgliosis are decreased in CSF-1R-cre+ mice compared to age-matched controls (Figures 5E–5G).

### NF-κB Regulates SOD1-G93A Microglial Conversion to an Inflammatory, Neurotoxic Phenotype

We hypothesized that the increased survival observed in SOD1-G93A; IKKβ[f/wt]; CSF-1R-cre+ mice was due to a dampened inflammatory microglial response. To characterize microglial phenotype, antibodies specific for CD68, iNOS, and CD86 were used to label microglia exhibiting an M1 inflammatory phenotype (Kigerl et al., 2009). As disease progresses, we and others have observed SOD1-G93A mice exhibit a robust induction in CD68-positive microglia that is greatest at ES (data not shown) (Beers et al., 2011b; Chiu et al., 2013). We found a marked reduction in the number of CD68 positive microglia in SOD1-G93A; IKKβ[f/wt]; CSF-1R-cre+ mice (112.4 ± 4.7 cells/section) compared to cre-negative controls (438.3 ± 13.4 cells/section) (Figures 6A and 6B). The number of iNOS+/Iba1+ cells/section was also significantly reduced from 251.1 ± 15.0 in controls to 47.8 ± 3.1 in mice with microglial NF-κB inhibition (Figures 6C and 6D). Following the same trend, mice with microglial NF-κB inhibition showed substantial reduction of CD86+/Iba1+ cells (97.8 ± 7.4 per section) compared to SOD1 controls (320.3 ± 15.6 cells per section) (Figures 6E and 6F). We did not

observe any alterations in the M2 markers CD206, arginase, or CD204 by immunohistochemistry, suggesting that while we inhibited M1 microglia, NF-κB inhibition did not promote an M2 phenotype (data not shown).

### NF-κB Activation Selectively in WT Microglia Is Sufficient to Induce MN Death In Vitro

We hypothesized that if NF-κB activation is the mechanism by which SOD1-G93A microglia induce MN death, constitutively activating NF-κB in WT microglia should be sufficient to induce MN death. To test this hypothesis, we isolated microglia from Rosa26-Stop[Flox]IKKβCA mice containing inducible constitutively active IKKβ (IKKβ CA). Postisolation, we infected microglia from these mice with an adenovirus expressing cre recombinase (Ad-cre) to induce transcription of constitutively active IKKβ (microglia termed IKKβCA) or Ad-RFP as control (microglia termed WT). After 12 hr in coculture with WT or IKKβCA microglia, we observed no difference in MN axon length or survival (Figure 7A). Interestingly, after 72 hr in coculture, IKKβCA microglia induced a 50% statistical decrease in MN survival compared to controls (Figures 7A and 7B). Live-imaging shows IKKβCA microglia rapidly inducing MN death (Movie S6). We confirmed NF-κB activation by ELISA, showing 1.7-fold greater phospho-p65/total p65 in IKKβCA microglia compared to WT (Figure 7C). Similarly, NF-κB-dependent luciferase activity normalized to renilla was 1.5-fold greater in IKKβCA microglia compared to WT (Figure S5A). Additionally, TNF-α levels increased 2.3-fold in cocultures with IKKβCA microglia compared to WT, which is comparable to TNF-α induction by SOD1-G93A microglia and characteristic of activated microglia (Figure S5B). Similarly, NO levels in IKKβCA microglia/MN coculture were 1.5-fold greater than WT (Figure S5C). These data suggest that constitutive NF-κB activation in microglia is sufficient to induce MN death independent of SOD1 mutations.

### NF-κB Regulates Microglial Activation to an Inflammatory, Neurotoxic Phenotype

Since we observed a reduction in inflammatory microglial markers CD68, iNOS, and CD86 with NF-κB inhibition, we hypothesized that NF-κB is required for microglial activation. Thus, we reasoned that selectively expressing constitutively active IKKβ (IKKβCA) in myeloid cells in vivo should induce an inflammatory state in WT microglia similar to that observed in ALS mice. To test this notion, we crossed mice expressing CSF-1R-cre to Rosa26-Stop[Flox]IKKβCA mice (termed IKKβCA). IKKβCA mice exhibited an 8.2-fold increase in phospho-p65 in lumbar spinal cord protein compared to cre-negative littermates, similar to levels in SOD1-G93A mice (Figure 7D). Enhanced microglial activation at 4 and 8 months in these mice also was associated with pronounced astrocytosis (Figure 7E). By 8 months, we observed a striking 40% decrease in ChAT+ MNs in the lumbar spinal cord (Figure 7F), which coincided with decreased mass and hind-limb grip strength in IKKβCA mice compared to WT littermates (Figures 7G and 7H). Thus, chronic activation of NF-κB signaling in myeloid cells creates the pathological features of ALS in the spinal cord (i.e., gliosis and MN death). While we focused on lumbar spinal MNs, it is likely other neurons and brain regions are affected by microglial activation in IKKβCA mice.
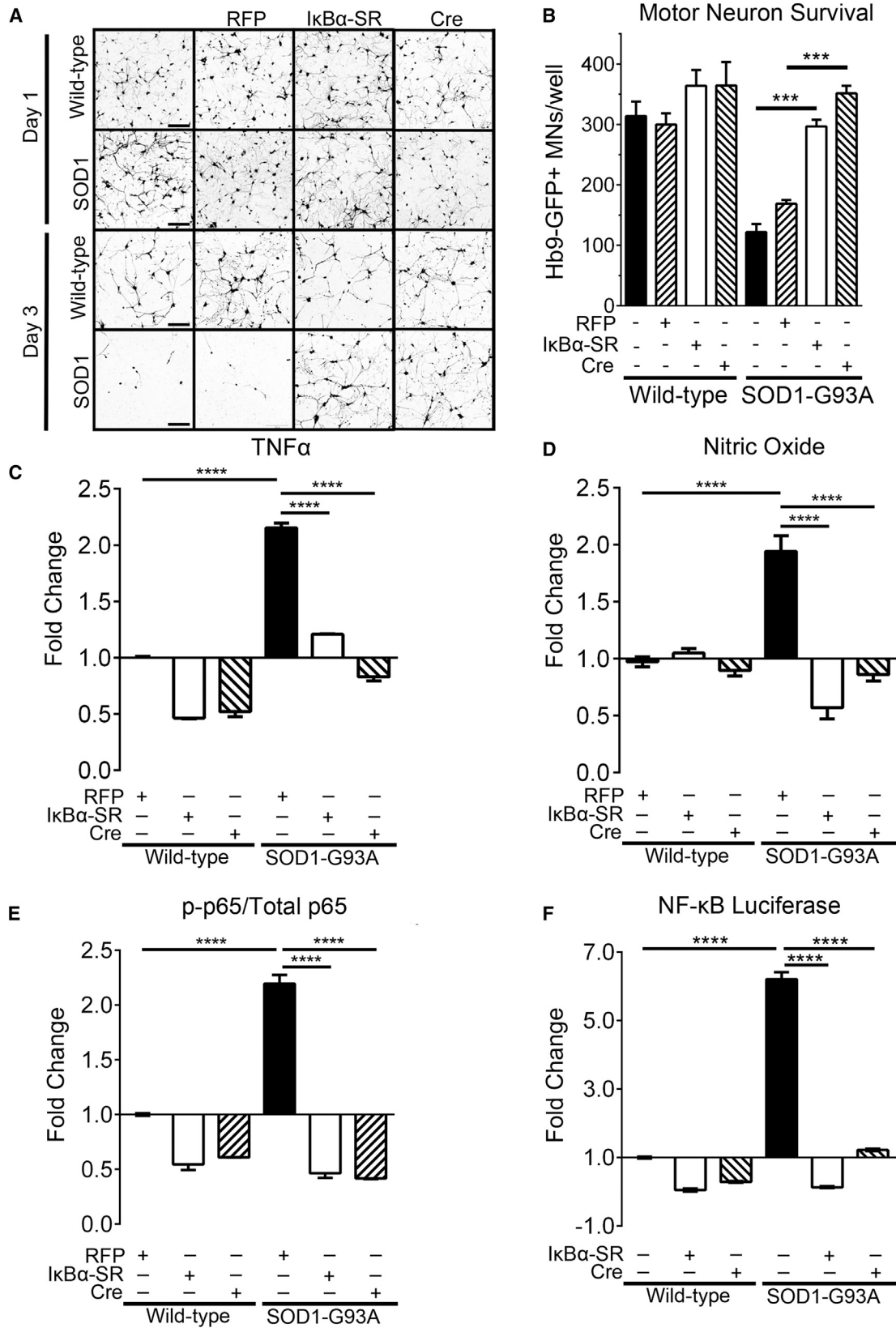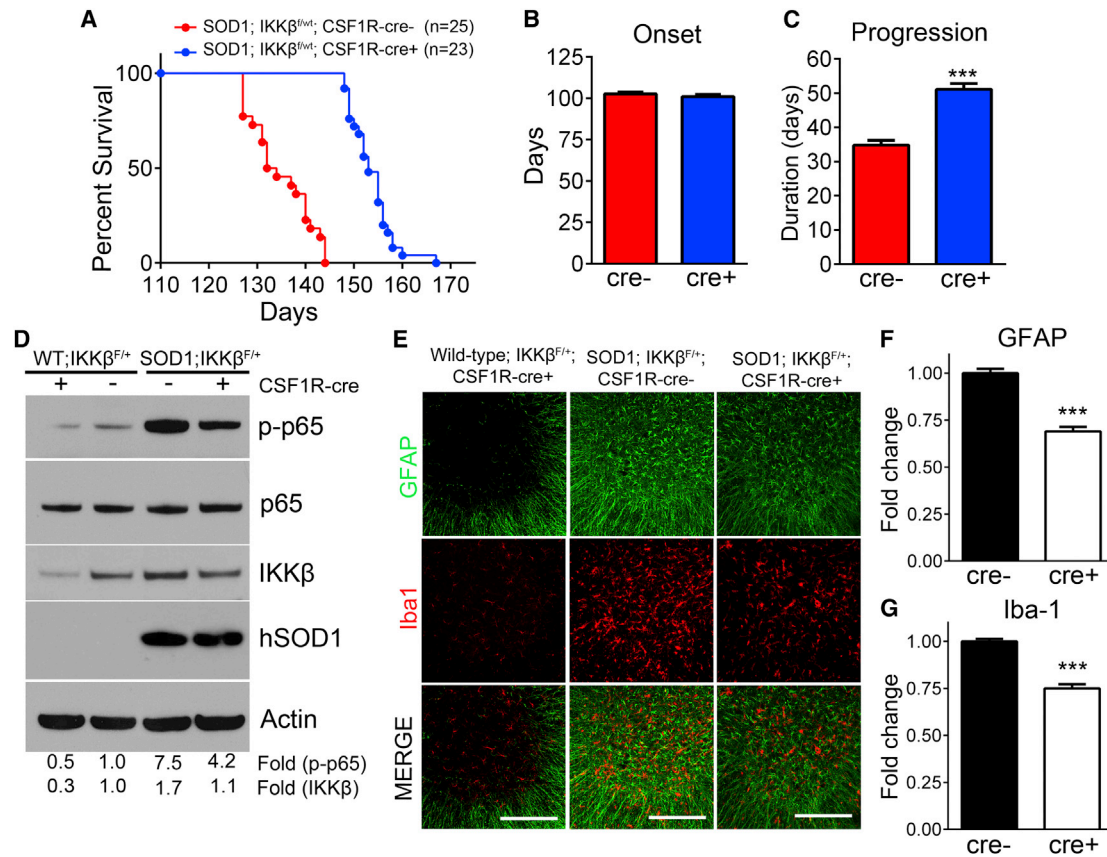
(legend on next page)

**Figure 5. SOD1-G93A Microglia Induce MN Death in an NF-κB-Dependent Mechanism In Vivo**

(A) Kaplan-Meier survival curve of SOD1-G93A; IKKβ$^{F/wt}$; CSF1R-cre− (n=22) and SOD1-G93A; IKKβ$^{F/wt}$; CSF-1R-cre+ mice (n=25). Median survival of SOD1-G93A; IKKβ$^{F/wt}$; CSF1R-cre− is 133 days and of SOD1-G93A; IKKβ$^{F/wt}$; CSF-1R-cre+ is 153 days. Mean survival for SOD1-G93A; IKKβ$^{F/wt}$; CSF1R-cre− is 134.9 ± 1.4 days and for SOD1-G93A; IKKβ$^{F/wt}$; CSF-1R-cre+ is 153.7 ± 0.9 days, with p<.0001.

(B) Disease onset determined by age at which peak weight was reached. SOD1-G93A; IKKβ$^{F/wt}$; CSF1R-cre-reached onset at 102.8 ± 1.1 days, and SOD1-G93A; IKKβ$^{F/wt}$; CSF1R-cre+ mice reached onset at 101.1 ± 1.3 days.

(C) Disease progression defined as time from disease onset to ES. SOD1-G93A; IKKβ$^{F/wt}$; CSF1R-cre− mean disease progression is 34.8 ± 1.4 days, and SOD1-G93A; IKKβ$^{F/wt}$; CSF1R-cre+ mean disease progression is 51.1 ± 1.7 days.

(D) Immunoblot of lumbar spinal cord protein isolated from WT; IKKβ$^{F/wt}$; CSF1R-cre+, WT; IKKβ$^{F/wt}$; CSF1R-cre-, and ES SOD1-G93A; IKKβ$^{F/wt}$; CSF1R-cre-, SOD1-G93A; IKKβ$^{F/wt}$ CSF1R-cre+ mice probed for phospho-p65 (top), total p65, IKKβ, human SOD1, and Actin (bottom). Fold change represents band intensities of phospho-p65 normalized to p65/Actin and IKKβ normalized to actin.

(E) Immunohistochemistry of Iba1-positive microglia (red) and GFAP-positive astrocytes (green) in the lumbar spinal cords of ES SOD1-G93A; IKKβ$^{F/wt}$ CSF1R-cre−, age-matched SOD1-G93A; IKKβf$^{/wt}$ CSF1R-cre+, and WT IKKβf$^{/wt}$ CSF1R-cre+ littermates. Scale bar indicate 200 μm.

(F and G) Quantification of GFAP and Iba-1 signal intensity in SOD1-G93A; IKKβ$^{F/wt}$ CSF1R-cre− and age-matched SOD1-G93A; IKKβf$^{/wt}$ CSF1R-cre+ immunohistochemistry in represented in (E). Error bars represent SEM. ***p< 0.001. See also Figure S4 and Movie S5.

To determine whether microglia in IKKβCA mice express activation markers, similar to those described above for activated (M1) microglia from SOD1-G93A mice, we analyzed microglia from the IKKβCA and cre-negative littermates for expression of CD68, iNOS, and CD86. A striking upregulation of CD68 and CD86 was observed in microglia from 4-month- and 8-month-old IKKβCA mice (Figures S6A and S6B). Microglia from IKKβCA mice also differed drastically from those found in WT controls exhibiting a deramified morphology with shorter, thickened processes shown by Iba-1 staining. We detected an increase in

**Figure 4. Adult SOD1-G93A Microglia Induce MN Death in an NF-κB-Dependent Mechanism In Vitro**

(A and B) Representative microscopic fields (A) and well counts (B) of Hb9-GFP+ MNs after 1 day (24 hr) and 3 days (72 hr) in coculture with WT or SOD1-G93A microglia not infected (black bars), infected with Ad-RFP (dashed bars), or infected with Ad-IκBα-SR (white bars). MNs cocultured with either WT; IKKβ$^{f/f}$ or SOD1-G93A; IKKβ$^{f/f}$ microglia infected with Ad-cre shown with dashed bars. Scale bar indicate 200 μm.

(C and D) Quantification of TNF-α (C) and nitric oxide (D) in the coculture medium by ELISA.

(E) Quantification of phospho-p65 by ELISA from microglial-MN cocultures. Phospho-p65 normalized to total p65 determined by ELISA.

(F) Luciferase assay of NF-κB activity in microglia. Firefly luciferase normalized to renilla luciferase. Error bars represent SEM. ****p< 0.0001; ***p< 0.001. See also Movies S1, S2, S3, and S4.
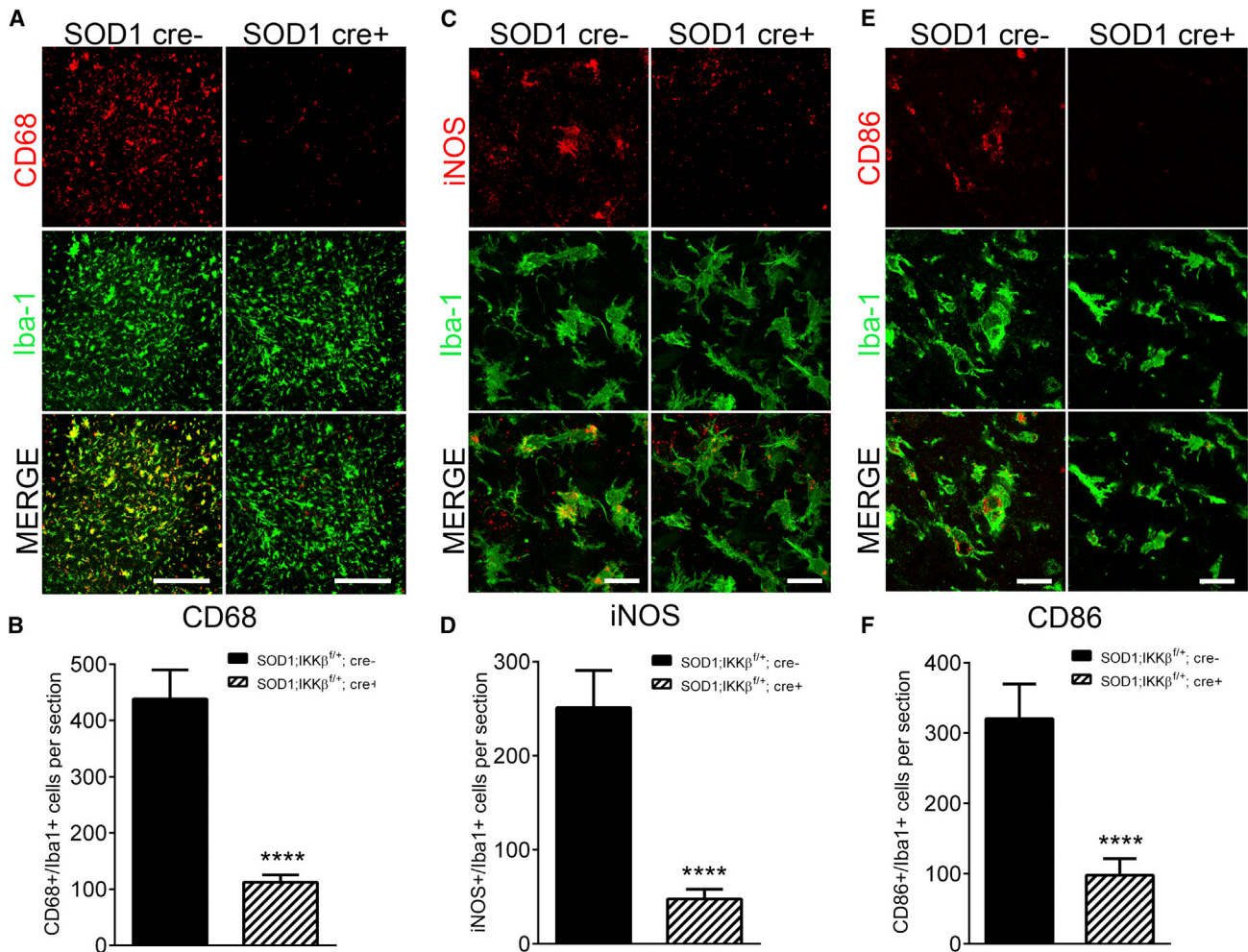
**Figure 6. NF-κB Inhibition in SOD1-G93A Microglia Impairs Microglial Activation to a Proinflammatory, Neurotoxic Phenotype**
(A and B) Immunohistochemistry (A) and quantification (B) of CD68 (red) and Iba1 (green) cells in lumbar spinal cord of disease-matched ES SOD1-G93A; IKKβ$^{F/wt}$ CSF1R-cre− and SOD1-G93A; IKKβ$^{F/wt}$ CSF1R-cre+ littermates. Scale bar indicates 200 μm.
(C and D) Immunohistochemistry (C) and quantification (D) of iNOS (red) and Iba1 (green) cells in lumbar spinal cord of disease-matched ES SOD1-G93A; IKKβ$^{F/wt}$ CSF1R-cre− and SOD1-G93A; IKKβ$^{F/wt}$ CSF1R-cre+ littermates. Scale bar indicates 20 μm.
(E and F) Immunohistochemistry (E) and quantification (F) of CD86 (red) and Iba1 (green) cells in lumbar spinal cord of disease-matched ES SOD1-G93A; IKKβ$^{F/wt}$ CSF1R-cre− and SOD1-G93A; IKKβ$^{F/wt}$ CSF1R-cre+ littermates. Scale bar indicates 20 μm. Error bars represent SEM. ****$p < 0.0001$.

iNOS+ microglia compared to WT controls at 8 months, but not at 4 months in IKKβCA mice (Figure S6C). Interestingly, we observed an increase in CD68 and CD86-positive microglia in 8 month WT controls compared to 4 month-old controls, which supports previous reports that microglial activation increases with aging (Norden and Godbout, 2013). These data suggest that chronic NF-κB activation induces an inflammatory (M1) microglia phenotype that causes MN death (Figures 8A and 8B).

## DISCUSSION

Landmark studies have shown selective removal of the causal mutant SOD1 gene from myeloid cells in the slow-progressing SOD1-G37R mice (Boillée et al., 2006) or repopulating the fast-progressing SOD1-G93A model with WT myeloid cells delays

disease progression (Beers et al., 2006). Therefore, we hypothesized that if NF-κB activation is a mechanism by which mutant SOD1 microglia mediates MN death in ALS, then disease progression will be substantially delayed in SOD1-G93A mice with microglial NF-κB inhibition. Mice homozygous for IKKβ (IKKβ$^{f/f}$), both SOD1 and WT, displayed serious immune dysfunction and could not be assessed for survival, so we generated SOD1; CSF1R-cre; IKKβ$^{F/+}$ heterozygous mice. Strikingly, heterozygous inhibition of NF-κB specifically in the myeloid lineage of the fast-progressing SOD1-G93A mouse model significantly delayed disease progression by 47%, resulting in a 20 day increase in survival. Therefore, our data extend those showing that ALS microglia contribute to MN death in a non-cell-autonomous mechanism, and we report that microglial-mediated MN death in ALS occurs through an NF-κB-dependent mechanism.
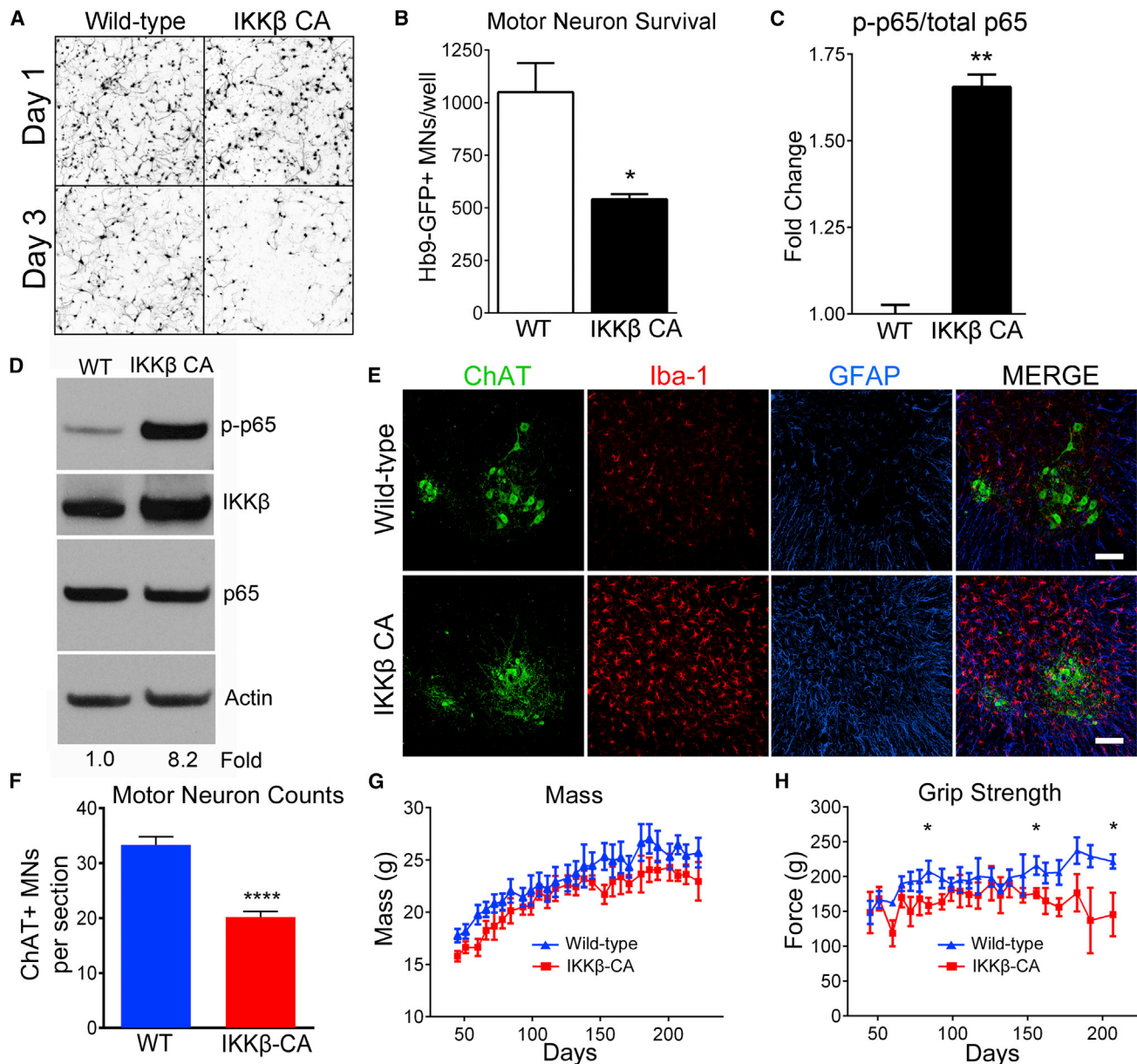
**Figure 7. NF-κB Activation in Wild-Type Microglia Induces MN Death**

(A and B) Representative microscopic fields (A) and counts (B) of Hb9-GFP+ MNs after 1 day (24 hr) and 3 days (72 hr) in coculture with WT microglia (white bar) or WT microglia with constitutively active IKKβ (IKKβCA) (black bar).

(C) Quantification of NF-κB activation (phospho-p65), normalized to total p65, both determined by ELISA.

(D) Immunoblot of lumbar spinal cord protein from WT and IKKβCA mice. The blot was probed for p-p65 (top), IKKβ (top middle), p65 (bottom middle), and actin (bottom). Phospho-p65 band intensities normalized to p65/Actin. Fold change determined by densitometry in Image J.

(E) Immunohistochemistry of lumbar spinal cords of WT and IKKβCA littermates at 8 months. Iba1-positive microglia (red), GFAP-positive astrocytes (blue), and ChAT-positive MNs (green). Scale bar indicates 100 μm.

(F) Counts of ChAT+ MNs in ventral horn of lumbar spinal cord from 8-month-old IKKβCA and WT littermates (n=3).

(G and H) Mass (G) and grip strength (H) of IKKβCA (n=6) and WT littermates (n=8). Error bars represent SEM. *p<0.05, **p<0.01, and ****p< 0.0001. See also Movie S6 and Figures S5 and S6.

To determine the extent by which NF-κB inhibition in microglia alters the neuroinflammatory hallmarks of ALS pathology, we analyzed lumbar sections for astrogliosis, microgliosis, and MN death. In SOD1-G93A; IKKβ$^{f/wt}$; CSF1R-cre+ mice with NF-κB inhibition in microglia, we observed a decrease in Iba-1 and GFAP compared to age-matched cre-negative control littermates, suggesting NF-κB inhibition delayed microglial activation and astrogliosis during disease progression. Additionally, we
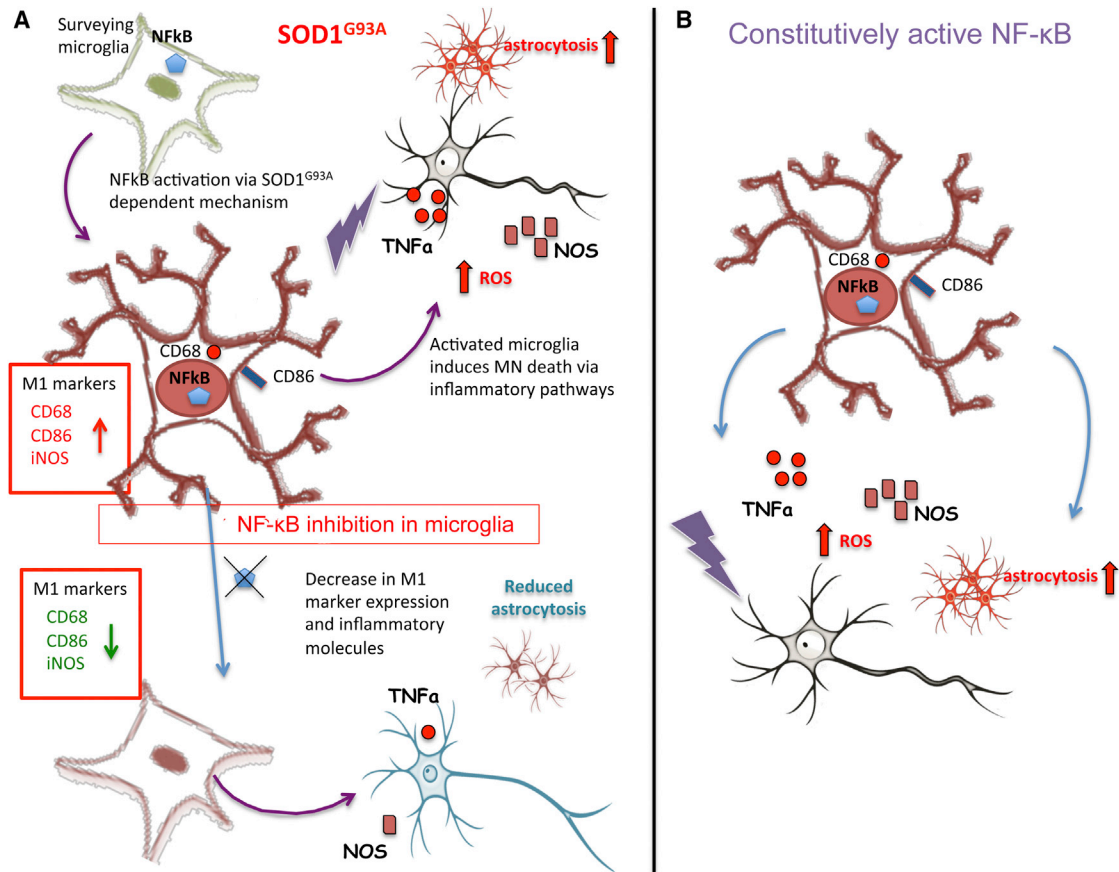
**Figure 8. The Classical NF-κB Pathway Mediates Microglial Activation and MN Death**

(A) Model of the mechanism by which SOD1-G93A microglia induce MN death in ALS. The NF-κB pathway is initiated in SOD1-G93A microglia by a SOD1-G93A-dependent mechanism leading to microglial activation and, subsequently, MN death via inflammatory pathways. Inhibition of microglial NF-κB in ALS mice blocks microglial activation, downregulates proinflammatory markers, and delays MN death.

(B) Model of IKKβCA mice in which NF-κB is constitutively active only in myeloid cells. Microglia in these mice exhibit a proinflammatory phenotype that induces MN death in a mutant SOD1-independent mechanism.

show NF-κB inhibition in astrocytes results in no benefit to ALS mice and in fact might be detrimental, which has been previously reported (Crosio et al., 2011). It is likely NF-κB might regulate important aspects of astrocyte function that are needed to support MNs under insult in ALS, which may explain why no benefit was observed with astroglial NF-κB inhibition in SOD1-G93A mice (Beattie et al., 2002; Bracchi-Ricard et al., 2008). These data suggest that astrocytes elicit a different non-cell-autonomous mechanism than microglia to induce MN death in ALS.

To determine whether the survival increase observed in SOD1-G93A; IKKβ[f/wt]; CSF-1R-cre+ mice was due to a dampened proinflammatory microglial response, we characterized microglia for known markers of microglial activation. Depending on the milieu in which they become activated, microglia differentiate into inflammatory (M1) and antiinflammatory (M2) effector cells with the potential to kill invading pathogens or neurons (M1), promote tissue repair, or dampen the immune response (M2) (Kigerl et al., 2009). These activation states were characterized initially in macrophages in vitro and likely represent an oversimplification of the in vivo functional potential of these cell types (Mosser and

Edwards, 2008; Ransohoff and Perry, 2009). Not surprisingly, ALS microglia have a unique proinflammatory (M1) gene signature compared to LPS-stimulated M1 microglia (Chiu et al., 2013). Previous reports showed an upregulation of genes in SOD1-G93A mice known to be expressed by inflammatory (or M1) microglia such as CD68, CD86, iNOS, TNF-α, NOX2, COX2, IL-6, and IL-1β, which increase with disease progression. In fact, SOD1-G93A; IKKβ[f/wt]; CSF-1R-cre+ mice exhibited a marked reduction in prototypic ALS microglia inflammatory markers such as CD68, CD86, and iNOS compared to cre-negative controls, suggesting proinflammatory M1 microglia play a central role in MN death in ALS (Figure 8A) (Beers et al., 2011a; Henkel et al., 2009; Zhao et al., 2004). Additionally, a recent report suggests infiltrating inflammatory monocytes contribute to MN death in ALS (Butovsky et al., 2012). Since CSF1R-cre is expressed in microglia and peripheral myeloid cells, we cannot exclude the possibility that the delay in disease progression we observe is due to NF-κB inhibition in peripheral macrophages or infiltrating monocytes. To further address the contribution of peripheral myeloid cells to ALS, new cre mouse strains or viral

vectors need to be developed that exclusively target microglia or peripheral macrophages/monocytes.

Since NF-κB activation is the mechanism by which SOD1-G93A microglia induce MN death, we hypothesized that constitutively activating NF-κB in WT microglia should be sufficient to induce MN death. Interestingly, microglia with constitutively active NF-κB rapidly induced a 50% decrease in MN survival in vitro compared to controls through a mechanism that is independent of mutant SOD1. Notably, 8-month-old IKKβCA mice exhibited a marked reduction in spinal MNs, accompanied by reduced weight and grip strength, indicative of muscle atrophy. Additionally, IKKβCA microglia showed increased levels of CD68, CD86, and iNOS compared to WT, suggesting NF-κB activation induces an inflammatory (M1) microglia phenotype that causes MN death (Figure 8B). While we cannot determine whether microglia or peripheral myeloid cells are inducing MN death, these data have strong implications for patients with familial mutations other than SOD1 and sporadic ALS patients. Recently, immunohistochemical studies showed that NF-κB is highly induced in microglia of sporadic patients, and those with mutation in the gene optineurin, a negative regulator of TNF-α, induced NF-κB activation that has been shown to cause ALS (Sako et al., 2012). Additionally, TDP-43 and FUS have been shown to be coactivators of NF-κB, and NF-κB inhibition in transgenic mice overexpressing mutant TDP-43 ameliorated the disease phenotype (Swarup et al., 2011; Uranishi et al., 2001). Furthermore, dysregulation of the NF-κB pathway in lymphoblastoid cell lines was identified by MetaCore analysis in both C9ORF72 patients and non-C9ORF72 patients (Ismail et al., 2013). Therefore, aberrant NF-κB activation could be driving the microglial inflammatory response in both familial and sporadic ALS and could be a universal therapeutic target for ALS.

However, targeting NF-κB is complicated due to its diverse functions in different cell types in the CNS and periphery. For example, NF-κB activation in glutamatergic neurons is involved in learning and memory, dendritic arborization, and axonal outgrowth (Gutierrez et al., 2005; Kaltschmidt et al., 2006). In the context of neurodegeneration, mice with selective inhibition of IKKβ in neuronal cells utilizing a CamkII cre-driver experienced more severe EAE symptoms and succumb to disease earlier due to their inability to induce neuronal expression of NF-κB-dependent neuroprotective and antiapoptotic genes (Emmanouil et al., 2009; Taoufik et al., 2011). Therefore, when targeting NF-κB in the CNS, cell-type specificity is likely required so that functional benefits achieved by dampening microglial inflammation are not masked by neuronal deficits induced by off-target neuronal NF-κB inhibition (Kaltschmidt and Kaltschmidt, 2009; Mattson and Meffert, 2006).

The data presented here clearly demonstrate that NF-κB is a promising therapeutic target for ALS. Heterozygous inhibition of NF-κB in microglia substantially delayed disease progression in the severe SOD1-G93A model. Strikingly, NF-κB activation in WT microglia causes MN death in vitro as well as in vivo, independent of mutant SOD1. This suggests traumatic events, environmental risks, or predisposing genetic factors that lead to chronic activation of NF-κB in microglia could trigger the pathogenic mechanism leading to MN death. The present data provide important insight on how microglia induce MN degeneration in a familial model of ALS, but even more interestingly, provide a therapeutic target for both familial and sporadic ALS patients.

## EXPERIMENTAL PROCEDURES

### Transgenic Mice

All procedures were performed in accordance with the NIH Guidelines on the care and use of vertebrate animals and approved by the Institutional Animal Care and Use Committee of the Research Institute at Nationwide Children's Hospital. Transgenic female B6SJ/L(SOD1-G93A)1Gur/J mice and nontransgenic littermates (Jackson Laboratories) were utilized for time course immunoblot studies, primary cell isolations, and breeding with other transgenic lines. SOD1 transgene copy number was confirmed by real-time PCR. See Supplemental Experimental Procedures for details.

### Primary Cell Isolations

Adult microglia were isolated as previously described with minor modifications (Moussaud and Draheim, 2010). Neonatal microglia were isolated from 3-day-old pups as previously described with minor modifications (Xiao et al., 2007). Adult primary astrocytes were isolated as previously described (Miranda et al., 2012). See Supplemental Experimental Procedures for details.

### Microglia/MN Coculture

Hb9-GFP+ MNs were plated in 96-well plates coated with laminin (5 μg/ml; Invitrogen) at a density of 6,000 cells per well. The day after, microglia were plated on top of MNs at a density of 35,000 cells per well in MN media (DMEM:F12; Invitrogen), 5% horse serum, 2% N2 (Invitrogen), 2% B27 (Invitrogen) + GDNF (10 ng/ml, Invitrogen), BDNF (10 ng/ml, Invitrogen), and CNTF (10 ng/ml, Invitrogen). The coculture plate was imaged each day by the IN Cell Analyzer 6000 (GE Healthcare). Images were processed and analyzed using IN Cell Developer Toolbox 1.9 and IN Cell Analyzer Workstation 3.7 software (GE Healthcare) to quantify number of surviving GFP+ MNs per well.

### Immunoblot Analysis

Cells and tissues were homogenized in Tissue Protein Extraction Reagent (Pierce) with EDTA, Complete protease inhibitor (Roche), and Phospho-STOP (Roche). Immunoblot analyses were performed as previously described (Foust et al., 2013). See Supplemental Experimental Procedures for details.

### Immunohistochemistry

Animals were deeply anesthetized with a lethal dose of xylazene/ketamine and perfused transcardially with saline, then 4% paraformaldehyde. Spinal cords were sectioned 40 μm thick using a vibrating blade microtome (Leica microsystems). Immunohistochemistry was performed as previously described (Foust et al., 2013). See Supplemental Experimental Procedures for details.

### Statistical Analyses

For all statistical tests, Graph Pad Prism 6 software (La Jolla) was used. Statistical analysis of mean differences between groups was performed by either Student's t test or one- or two-way ANOVA, followed by a Bonferroni post hoc analysis depending on the number of variables and time-points in each experiment. All p values and n values are indicated in figure legends.

## SUPPLEMENTAL INFORMATION

Supplemental Information includes six figures, two tables, six movies, and Supplemental Experimental Procedures and can be found with this article online at http://dx.doi.org/10.1016/j.neuron.2014.01.013.

## ACKNOWLEDGEMENTS

## REFERENCES

Alexianu, M.E., Kozovska, M., and Appel, S.H. (2001). Immune reactivity in a mouse model of familial ALS correlates with disease progression. Neurology 57, 1282–1289.

Almer, G., Kikuchi, H., Teismann, P., and Przedborski, S. (2006). Is prostaglandin E(2) a pathogenic factor in amyotrophic lateral sclerosis? Ann. Neurol. 59, 980–983.

Beattie, E.C., Stellwagen, D., Morishita, W., Bresnahan, J.C., Ha, B.K., Von Zastrow, M., Beattie, M.S., and Malenka, R.C. (2002). Control of synaptic strength by glial TNFalpha. Science 295, 2282–2285.

Beers, D.R., Henkel, J.S., Xiao, Q., Zhao, W., Wang, J., Yen, A.A., Siklós, L., McKercher, S.R., and Appel, S.H. (2006). Wild-type microglia extend survival in PU.1 knockout mice with familial amyotrophic lateral sclerosis. Proc. Natl. Acad. Sci. USA 103, 16021–16026.

Beers, D.R., Henkel, J.S., Zhao, W., Wang, J., Huang, A., Wen, S., Liao, B., and Appel, S.H. (2011a). Endogenous regulatory T lymphocytes ameliorate amyotrophic lateral sclerosis in mice and correlate with disease progression in patients with amyotrophic lateral sclerosis. Brain 134, 1293–1314.

Beers, D.R., Zhao, W., Liao, B., Kano, O., Wang, J., Huang, A., Appel, S.H., and Henkel, J.S. (2011b). Neuroinflammation modulates distinct regional and temporal clinical responses in ALS mice. Brain Behav. Immun. 25, 1025–1035.

Boillée, S., Yamanaka, K., Lobsiger, C.S., Copeland, N.G., Jenkins, N.A., Kassiotis, G., Kollias, G., and Cleveland, D.W. (2006). Onset and progression in inherited ALS determined by motor neurons and microglia. Science 312, 1389–1392.

Bracchi-Ricard, V., Brambilla, R., Levenson, J., Hu, W.-H., Bramwell, A., Sweatt, J.D., Green, E.J., and Bethea, J.R. (2008). Astroglial nuclear factor-kappaB regulates learning and memory and synaptic plasticity in female mice. J. Neurochem. 104, 611–623.

Butovsky, O., Siddiqui, S., Gabriely, G., Lanser, A.J., Dake, B., Murugaiyan, G., Doykan, C.E., Wu, P.M., Gali, R.R., Iyer, L.K., et al. (2012). Modulating inflammatory monocytes with a unique microRNA gene signature ameliorates murine ALS. J. Clin. Invest. 122, 3063–3087.

Chiu, I.M., Morimoto, E.T.A., Goodarzi, H., Liao, J.T., O'Keeffe, S., Phatnani, H.P., Muratet, M., Carroll, M.C., Levy, S., Tavazoie, S., et al. (2013). A neurodegeneration-specific gene-expression signature of acutely isolated microglia from an amyotrophic lateral sclerosis mouse model. Cell Rep. 4, 385–401.

Clement, A.M., Nguyen, M.D., Roberts, E.A., Garcia, M.L., Boillée, S., Rule, M., McMahon, A.P., Doucette, W., Siwek, D., Ferrante, R.J., et al. (2003). Wild-type nonneuronal cells extend survival of SOD1 mutant motor neurons in ALS mice. Science 302, 113–117.

Crosio, C., Valle, C., Casciati, A., Iaccarino, C., and Carrì, M.T. (2011). Astroglial inhibition of NF-κB does not ameliorate disease onset and progression in a mouse model for amyotrophic lateral sclerosis (ALS). PLoS ONE 6, e17187.

Di Giorgio, F.P., Carrasco, M.A., Siao, M.C., Maniatis, T., and Eggan, K. (2007). Non-cell autonomous effect of glia on motor neurons in an embryonic stem cell-based ALS model. Nat. Neurosci. 10, 608–614.

Di Giorgio, F.P., Boulting, G.L., Bobrowicz, S., and Eggan, K.C. (2008). Human embryonic stem cell-derived motor neurons are sensitive to the toxic effect of glial cells carrying an ALS-causing mutation. Cell Stem Cell 3, 637–648.

Emmanouil, M., Taoufik, E., Tseveleki, V., Vamvakas, S.-S., Tselios, T., Karin, M., Lassmann, H., and Probert, L. (2009). Neuronal I kappa B kinase beta protects mice from autoimmune encephalomyelitis by mediating neuroprotective and immunosuppressive effects in the central nervous system. J. Immunol. 183, 7877–7889.

Erblich, B., Zhu, L., Etgen, A.M., Dobrenis, K., and Pollard, J.W. (2011). Absence of colony stimulation factor-1 receptor results in loss of microglia, disrupted brain development and olfactory deficits. PLoS ONE 6, e26317.

Foust, K.D., Nurre, E., Montgomery, C.L., Hernandez, A., Chan, C.M., and Kaspar, B.K. (2009). Intravascular AAV9 preferentially targets neonatal neurons and adult astrocytes. Nat. Biotechnol. 27, 59–65.

Foust, K.D., Salazar, D.L., Likhite, S., Ferraiuolo, L., Ditsworth, D., Ilieva, H., Meyer, K., Schmelzer, L., Braun, L., Cleveland, D.W., et al. (2013). Therapeutic AAV9-mediated Suppression of Mutant SOD1 Slows Disease Progression and Extends Survival in Models of Inherited ALS. Molecular Therapy. 21, 2148–2159.

Ghosh, S., and Karin, M. (2002). Missing pieces in the NF-kappaB puzzle. Cell 109 (Suppl), S81–S96.

Gowing, G., Dequen, F., Soucy, G., and Julien, J.-P. (2006). Absence of tumor necrosis factor-alpha does not affect motor neuron disease caused by superoxide dismutase 1 mutations. J. Neurosci. 26, 11397–11402.

Gutierrez, H., Hale, V.A., Dolcet, X., and Davies, A. (2005). NF-kappaB signalling regulates the growth of neural processes in the developing PNS and CNS. Development 132, 1713–1726.

Haidet-Phillips, A.M., Hester, M.E., Miranda, C.J., Meyer, K., Braun, L., Frakes, A., Song, S., Likhite, S., Murtha, M.J., Foust, K.D., et al. (2011). Astrocytes from familial and sporadic ALS patients are toxic to motor neurons. Nat. Biotechnol. 29, 824–828.

Hall, E.D., Oostveen, J.A., and Gurney, M.E. (1998). Relationship of microglial and astrocytic activation to disease onset and progression in a transgenic model of familial ALS. Glia 23, 249–256.

Hayden, M.S., and Ghosh, S. (2008). Shared principles in NF-kappaB signaling. Cell 132, 344–362.

Henkel, J.S., Beers, D.R., Zhao, W., and Appel, S.H. (2009). Microglia in ALS: the good, the bad, and the resting. J. Neuroimmune Pharmacol. 4, 389–398.

Ismail, A., Cooper-Knock, J., Highley, J.R., Milano, A., Kirby, J., Goodall, E., Lowe, J., Scott, I., Constantinescu, C.S., Walters, S.J., et al. (2013). Concurrence of multiple sclerosis and amyotrophic lateral sclerosis in patients with hexanucleotide repeat expansions of C9ORF72. J. Neurol. Neurosurg. Psychiatry 84, 79–87.

Kaltschmidt, B., and Kaltschmidt, C. (2009). NF-kappaB in the nervous system. Cold Spring Harb. Perspect. Biol. 1, a001271.

Kaltschmidt, B., Ndiaye, D., Korte, M., Pothion, S., Arbibe, L., Prüllage, M., Pfeiffer, J., Lindecke, A., Staiger, V., Israël, A., et al. (2006). NF-kappaB regulates spatial memory formation and synaptic plasticity through protein kinase A/CREB signaling. Mol. Cell. Biol. 26, 2936–2946.

Kawamata, T., Akiyama, H., Yamada, T., and McGeer, P.L. (1992). Immunologic reactions in amyotrophic lateral sclerosis brain and spinal cord tissue. Am. J. Pathol. 140, 691–707.

Kigerl, K.A., Gensel, J.C., Ankeny, D.P., Alexander, J.K., Donnelly, D.J., and Popovich, P.G. (2009). Identification of two distinct macrophage subsets with divergent effects causing either neurotoxicity or regeneration in the injured mouse spinal cord. J. Neurosci. 29, 13435–13444.

Lerman, B.J., Hoffman, E.P., Sutherland, M.L., Bouri, K., Hsu, D.K., Liu, F.-T., Rothstein, J.D., and Knoblach, S.M. (2012). Deletion of galectin-3 exacerbates microglial activation and accelerates disease progression and demise in a SOD1(G93A) mouse model of amyotrophic lateral sclerosis. Brain Behav. 2, 563–575.

Li, Z.-W., Omori, S.A., Labuda, T., Karin, M., and Rickert, R.C. (2003). IKK beta is required for peripheral B cell survival and proliferation. J. Immunol. 170, 4630–4637.

Magness, S.T., Jijon, H., Van Houten Fisher, N., Sharpless, N.E., Brenner, D.A., and Jobin, C. (2004). In vivo pattern of lipopolysaccharide and anti-CD3-induced NF-kappa B activation using a novel gene-targeted enhanced GFP reporter gene mouse. J. Immunol. 173, 1561–1570.

Mantovani, S., Garbelli, S., Pasini, A., Alimonti, D., Perotti, C., Melazzini, M., Bendotti, C., and Mora, G. (2009). Immune system alterations in sporadic

amyotrophic lateral sclerosis patients suggest an ongoing neuroinflammatory process. J. Neuroimmunol. *210*, 73–79.

Marchetto, M.C.N., Muotri, A.R., Mu, Y., Smith, A.M., Cezar, G.G., and Gage, F.H. (2008). Non-cell-autonomous effect of human SOD1 G37R astrocytes on motor neurons derived from human embryonic stem cells. Cell Stem Cell *3*, 649–657.

Maruyama, H., Morino, H., Ito, H., Izumi, Y., Kato, H., Watanabe, Y., Kinoshita, Y., Kamada, M., Nodera, H., Suzuki, H., et al. (2010). Mutations of optineurin in amyotrophic lateral sclerosis. Nature *465*, 223–226.

Mattson, M.P., and Meffert, M.K. (2006). Roles for NF-kappaB in nerve cell survival, plasticity, and disease. Cell Death Differ. *13*, 852–860.

Miranda, C.J., Braun, L., Jiang, Y., Hester, M.E., Zhang, L., Riolo, M., Wang, H., Rao, M., Altura, R.A., and Kaspar, B.K. (2012). Aging brain microenvironment decreases hippocampal neurogenesis through Wnt-mediated survivin signaling. Aging Cell *11*, 542–552.

Mosser, D.M., and Edwards, J.P. (2008). Exploring the full spectrum of macrophage activation. Nat. Rev. Immunol. *8*, 958–969.

Moussaud, S., and Draheim, H.J. (2010). A new method to isolate microglia from adult mice and culture them for an extended period of time. J. Neurosci. Methods *187*, 243–253.

Nagai, M., Re, D.B., Nagata, T., Chalazonitis, A., Jessell, T.M., Wichterle, H., and Przedborski, S. (2007). Astrocytes expressing ALS-linked mutated SOD1 release factors selectively toxic to motor neurons. Nat. Neurosci. *10*, 615–622.

Nguyen, M.D., Julien, J.P., and Rivest, S. (2001). Induction of proinflammatory molecules in mice with amyotrophic lateral sclerosis: no requirement for proapoptotic interleukin-1beta in neurodegeneration. Ann. Neurol. *50*, 630–639.

Norden, D.M., and Godbout, J.P. (2013). Review: microglia of the aged brain: primed to be activated and resistant to regulation. Neuropathol. Appl. Neurobiol. *39*, 19–34.

Park, J.M., Greten, F.R., Li, Z.-W., and Karin, M. (2002). Macrophage apoptosis by anthrax lethal factor through p38 MAP kinase inhibition. Science *297*, 2048–2051.

Philips, T., and Robberecht, W. (2011). Neuroinflammation in amyotrophic lateral sclerosis: role of glial activation in motor neuron disease. Lancet Neurol. *10*, 253–263.

Ransohoff, R.M., and Perry, V.H. (2009). Microglial physiology: unique stimuli, specialized responses. Annu. Rev. Immunol. *27*, 119–145.

Rosen, D.R., Siddique, T., Patterson, D., Figlewicz, D.A., Sapp, P., Hentati, A., Donaldson, D., Goto, J., O'Regan, J.P., Deng, H.X., et al. (1993). Mutations in Cu/Zn superoxide dismutase gene are associated with familial amyotrophic lateral sclerosis. Nature *362*, 59–62.

Ruocco, M.G., Maeda, S., Park, J.M., Lawrence, T., Hsu, L.-C., Cao, Y., Schett, G., Wagner, E.F., and Karin, M. (2005). IkappaB kinase (IKK)beta, but not IKKalpha, is a critical mediator of osteoclast survival and is required for inflammation-induced bone loss. J. Exp. Med. *201*, 1677–1687.

Sako, W., Ito, H., Yoshida, M., Koizumi, H., Kamada, M., Fujita, K., Hashizume, Y., Izumi, Y., and Kaji, R. (2012). Nuclear factor κ B expression in patients with sporadic amyotrophic lateral sclerosis and hereditary amyotrophic lateral sclerosis with optineurin mutations. Clin. Neuropathol. *31*, 418–423.

Sasmono, R.T., and Williams, E. (2012). Generation and characterization of MacGreen mice, the Cfs1r-EGFP transgenic mice. Methods Mol. Biol. *844*, 157–176.

Sasmono, R.T., Oceandy, D., Pollard, J.W., Tong, W., Pavli, P., Wainwright, B.J., Ostrowski, M.C., Himes, S.R., and Hume, D.A. (2003). A macrophage colony-stimulating factor receptor-green fluorescent protein transgene is expressed throughout the mononuclear phagocyte system of the mouse. Blood *101*, 1155–1163.

Son, M., Fathallah-Shaykh, H.M., and Elliott, J.L. (2001). Survival in a transgenic model of FALS is independent of iNOS expression. Ann. Neurol. *50*, 273.

Swarup, V., Phaneuf, D., Dupré, N., Petri, S., Strong, M., Kriz, J., and Julien, J.-P. (2011). Deregulation of TDP-43 in amyotrophic lateral sclerosis triggers nuclear factor κB-mediated pathogenic pathways. J. Exp. Med. *208*, 2429–2447.

Taoufik, E., Tseveleki, V., Chu, S.Y., Tselios, T., Karin, M., Lassmann, H., Szymkowski, D.E., and Probert, L. (2011). Transmembrane tumour necrosis factor is neuroprotective and regulates experimental autoimmune encephalomyelitis via neuronal nuclear factor-kappaB. Brain *134*, 2722–2735.

Turner, M.R., Cagnin, A., Turkheimer, F.E., Miller, C.C.J., Shaw, C.E., Brooks, D.J., Leigh, P.N., and Banati, R.B. (2004). Evidence of widespread cerebral microglial activation in amyotrophic lateral sclerosis: an [11C](R)-PK11195 positron emission tomography study. Neurobiol. Dis. *15*, 601–609.

Uranishi, H., Tetsuka, T., Yamashita, M., Asamitsu, K., Shimizu, M., Itoh, M., and Okamoto, T. (2001). Involvement of the pro-oncoprotein TLS (translocated in liposarcoma) in nuclear factor-kappa B p65-mediated transcription as a coactivator. J. Biol. Chem. *276*, 13395–13401.

Vallabhapurapu, S., and Karin, M. (2009). Regulation and function of NF-kappaB transcription factors in the immune system. Annu. Rev. Immunol. *27*, 693–733.

Wang, C.Y., Cusack, J.C., Jr., Liu, R., and Baldwin, A.S., Jr. (1999). Control of inducible chemoresistance: enhanced anti-tumor therapy through increased apoptosis by inhibition of NF-kappaB. Nat. Med. *5*, 412–417.

Wichterle, H., Lieberam, I., Porter, J.A., and Jessell, T.M. (2002). Directed differentiation of embryonic stem cells into motor neurons. Cell *110*, 385–397.

Xiao, Q., Zhao, W., Beers, D.R., Yen, A.A., Xie, W., Henkel, J.S., and Appel, S.H. (2007). Mutant SOD1(G93A) microglia are more neurotoxic relative to wild-type microglia. J. Neurochem. *102*, 2008–2019.

Yamanaka, K., Chun, S.J., Boillee, S., Fujimori-Tonou, N., Yamashita, H., Gutmann, D.H., Takahashi, R., Misawa, H., and Cleveland, D.W. (2008). Astrocytes as determinants of disease progression in inherited amyotrophic lateral sclerosis. Nat. Neurosci. *11*, 251–253.

Zhao, W., Xie, W., Le, W., Beers, D.R., He, Y., Henkel, J.S., Simpson, E.P., Yen, A.A., Xiao, Q., and Appel, S.H. (2004). Activated microglia initiate motor neuron injury by a nitric oxide and glutamate-mediated mechanism. J. Neuropathol. Exp. Neurol. *63*, 964–977.

Zhuo, L., Theis, M., Alvarez-Maya, I., Brenner, M., Willecke, K., and Messing, A. (2001). hGFAP-cre transgenic mice for manipulation of glial and neuronal function in vivo. Genesis *31*, 85–94.